Development of a Novel Combined Absorption Cycle for Power Generation and Refrigeration[1]

Na Zhang[2]
Institute of Engineering Thermophysics,
Chinese Academy of Sciences,
Beijing 100080, P. R. China
e-mail: zhangna@mail.etp.ac.cn

Noam Lior
Department of Mechanical Engineering and
Applied Mechanics,
University of Pennsylvania,
Philadelphia, PA 19104-6315

Cogeneration can improve energy utilization efficiency significantly. In this paper, a new ammonia-water system is proposed for the cogeneration of refrigeration and power. The plant operates in a parallel combined cycle mode with an ammonia-water Rankine cycle and an ammonia refrigeration cycle, interconnected by absorption, separation, and heat transfer processes. The performance was evaluated by both energy and exergy efficiencies, with the latter providing good guidance for system improvement. The influences of the key parameters, which include the basic working solution concentration, the cooling water temperature, and the Rankine cycle turbine inlet parameters on the cycle performance, have been investigated. It is found that the cycle has a good thermal performance, with energy and exergy efficiencies of 27.7% and 55.7%, respectively, for the base-case studied (having a maximum cycle temperature of 450°C*). Comparison with the conventional separate generation of power and refrigeration having the same outputs shows that the energy consumption of the cogeneration cycle is markedly lower. A brief review of desirable properties of fluid pairs for such cogeneration cycles was made, and detailed studies for finding new fluid pairs and the impact of their properties on cogeneration system performance are absent and are very recommended.* [DOI: 10.1115/1.2751506]

1 Introduction

Gas-steam combined cycles have the highest energy efficiency among common power plants, with the biggest exergy losses occurring in the combustion process and in the heat transfer process between the topping Brayton cycle and the bottoming Rankine cycle (cf. [1]). An approach to reduce the exergy loss in the heat transfer process from a variable temperature heat source (such as the turbine exhaust gas in this topping cycle) is to concurrently also vary the temperature of the heat sink and thus make the temperature difference between the heat source and sink more uniform along the heat exchanger. This can be accomplished in a number of ways, such as by using a multi-pressure boiler in the Rankine cycle (that is the heat sink), by employment of a supercritical bottoming cycle, or by using binary-component working fluids that exhibit a variable boiling temperature during the boiling process.

Maloney and Robertson [2] introduced the use of an ammonia/water mixture (a widely used working fluid in refrigeration machines) as the working fluid in an absorption power cycle. In the combined power cycle proposed by Kalina [3], an ammonia/water mixture was employed as the working fluid in the bottoming cycle, and was found [4] to produce under certain conditions more power than the Maloney and Robertson cycle. Others have also analyzed such binary cycles [5,6] and proposed different methods for producing higher power outputs, such as integrations with a liquefied natural gas (LNG) evaporation process [5] or with an absorption refrigeration unit [6].

All the above-mentioned systems have power as their only usable output. In this paper we propose and explore a cogeneration system that produces both refrigeration and power.

Compared to the separate generation of power and cooling or heating, cogeneration can have an arrangement of energy and exergy "flows" within the system that results in lower fuel consumption [7]. Goswami et al. [8] proposed a combined power/refrigeration cycle using ammonia-water as the mixed working fluids, and investigated its performance [9–14]. Their analysis made under idealized conditions (neglecting all the irreversibilities) yielded energy and exergy efficiencies of 23.6% and 65%, respectively (when operated between the top and bottom temperatures of 400 K and 280 K). In their system, the ammonia vapor from a rectifier unit, which is about 20% of the total mass flow, first expands in a turbine to generate power and then the cold turbine exhaust provides cooling by transferring only sensible heat to the chilled water. The cooling capacity drops with the increase of the turbine inlet temperature, hence the system was mainly intended to be operated by low temperature heat sources. Most (~80%) of the working fluid mass flow is recycled as the absorbent in this system and therefore leads to relatively low outputs of power and refrigeration per unit working fluid mass flow rate. Zheng et al. [15] also proposed an absorption power and cooling (APC) combined cycle based on the Kalina cycle. To produce almost pure ammonia, a rectifier was used to replace the flash tank in the Kalina cycle. The outflow from the top of the rectifier is throttled by a valve and then produces refrigeration before mixing with the main stream. An energy efficiency of 24.2% and an exergy efficiency of 37.3% were reported with the turbine inlet parameters of 350°C/50 bar. Several variants of such absorption cogeneration cycles have also been described in a number of patents (cf. [16–18]).

A new ammonia-water system is proposed in this paper, for the cogeneration of refrigeration and power. The plant operates in a parallel combined cycle mode with an ammonia-water Rankine cycle and an ammonia refrigeration cycle, interconnected by the absorption, separation, and heat transfer processes. The perfor-

[1]This paper is a revision of ASME paper IMECE2004-60692 published at the IMECE 2004, Anaheim, CA. It corrects a few noncritical errors found in the IMECE paper and expands the analysis.

[2]Corresponding author.

Contributed by the Advanced Energy Systems Division of ASME for publication in the JOURNAL OF ENERGY RESOURCES TECHNOLOGY. Manuscript received March 7, 2006; final manuscript received July 23, 2006. Review conducted by Abdi Zaltash. Paper presented at the 2004 ASME International Mechanical Engineering Congress (IMECE2004), November 13–19, 2004, Anaheim, California, USA.

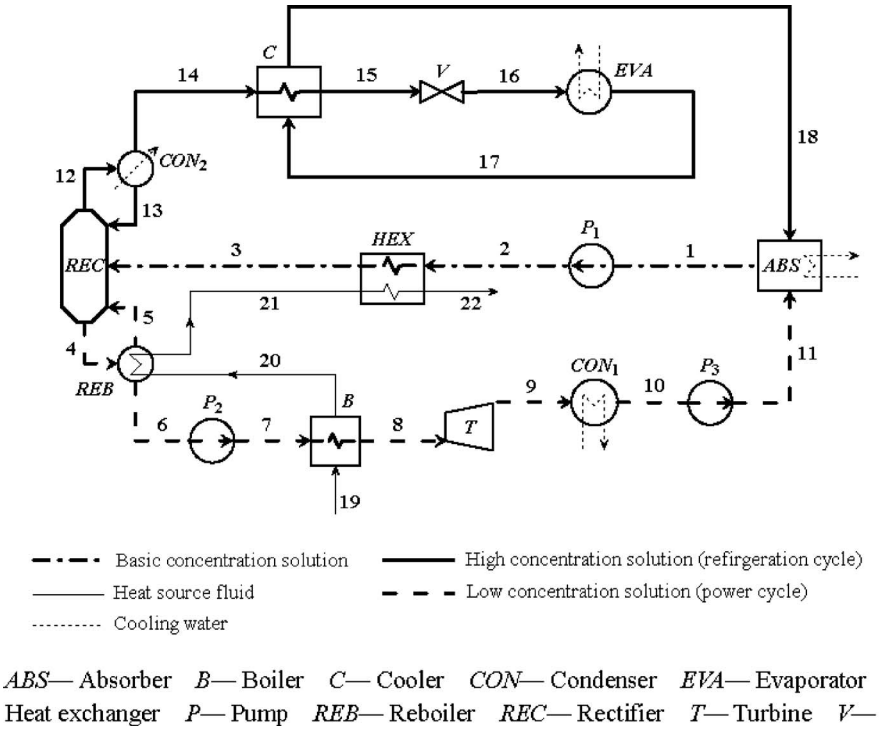

ABS— Absorber *B*— Boiler *C*— Cooler *CON*— Condenser *EVA*— Evaporator *HEX*— Heat exchanger *P*— Pump *REB*— Reboiler *REC*— Rectifier *T*— Turbine *V*— Valve

Fig. 1 The flow sheet of the combined power/refrigeration cycle

mance is evaluated by both the energy and exergy efficiencies and is compared with conventional separate cycles for generation of power and refrigeration.

The Cycle Configuration Description

An important motivation in the development of the cycle proposed and analyzed in this paper was the recognition that proper operation of the absorption cooling cycle requires the generator to operate at a significantly higher pressure than the absorber (here the pressure ratio is ~7), and that the weak solution flow (which is about 80% of total work fluid mass flow rate) from the generator to the absorber is just throttled for creating this pressure drop. In the base case system analyzed below (Fig. 1 and Tables 1–3), the results show that the replacement of the throttling by power generation is significant, having energy and exergy, (H_6-H_{11}) and $[(H_6-H_{11})-T_a(H_6-H_{11})]$, values, respectively, of 15% and 8.5% of the total cycle heat input and exergy input. Introduction of a steam-driven power generation system in lieu of the throttling valve, with heat addition to vaporize the weak solution, allows generation of power alongside with the refrigeration produced by the absorption system. Furthermore, judicious design allows also the use of streams that are not cold enough for refrigeration use, but are colder than the turbine exhaust, to increase the power generation by cooling the turbine exhaust to a lower temperature and thus to a lower condensation pressure.

Unlike the conventional gas-steam combined cycle, the two subcycles in the proposed power/refrigeration combined cycle use the same working fluid, a mixture of ammonia and water, but with different concentrations. The combined cycle configuration can be varied according to the relative positions and interaction of the two subcycles.

One basic cycle configuration is proposed in this paper as the parallel combined cycle. The cycle layout is shown in Fig. 1. The power cycle can be identified as 6-7-8-9-10-11-1. The refrigeration cycle is 14-15-16-17-18-1. They connect together in the process 1-2-3-4/12-···-6/14. A rectifier is needed to separate the feeding stream into the top ammonia rich outflow (12) and the bottom ammonia weak outflow (4). A reboiler and reflux are necessary at the bottom and the top of the rectifier, respectively, to maintain the continuing exchange of mass and heat in each rectifier stage. Correspondingly, the working fluid has basically three concentration levels: the basic concentration solution in the pro-

Table 1 Main assumptions for the base-case calculation

Cycle parameter	Basic working solution ammonia mass fraction X (kg NH_3/kg mixture)	0.3
	Cooling water temperature t_w (°C)	30.0
Ambient state	Temperature t_a (°C)	25.0
	Pressure p_a (bar)	1.013
Evaporator (*EVA*)	Pressure p_{EVA} (bar)	1.96
	Pressure loss (%)	3.0
	Outlet vapor fraction *VF*	0.9
Absorber (*ABS*)	Absorption pressure (bar)	1.84
	Pressure loss (%)	3.0
Turbine (*T*)	Inlet temperature t_8 (°C)	450.0
	Inlet pressure p_8 (bar)	52.4
	Backpressure p_b (bar)	0.242
	Isentropic efficiency (%)	87
Rectifier (*REC*)	Theoretical stage number	6
	Molar reflux ratio *RR*	0.3
	Operation pressure p_{REC} (bar)	14
	Pressure loss (%)	3.0
Reboiler (*REB*)	Outlet temperature t_{REB} (°C)	160
Heat exchangers. (*B*, *REB*, *HEX*, *CON*, *C*, *ABS*)	Pinch point temperature difference ΔT_P (K)	5 15 (if one side is air)
	Pressure loss (%)	1.0–3.0
Pumps (*P*)	Efficiency (%)	75

Table 2 The cycle stream states

	No.	t (°C)	p (bar)	Vapor fraction	h (kJ/kg)	s (kJ/kg·K)	m (kg/s)	X	
Working fluid	1	45.1	1.79	0	−12,469.9	−9.7	1	0.3	
	3	117.9	14.42	0	−12,030.1	−8.535	1	0.3	
	6	160	14	0	−13,907.6	−7.606	0.789	0.118	
	8	450	52.4	1	−11,356.4	−2.794	0.789	0.118	
	9	61.3	0.242	0.919	−12,286	−2.378	0.789	0.118	
	10	35	0.235	0	−14,566.4	−9.318	0.789	0.118	
	14	37.4	14	0	−4076.82	−10.697	0.211	0.98	
	15	−5.1	13.58	0	−4314.23	−11.486	0.211	0.98	
	16	−18.8	1.96	0.053	−4314.22	−11.448	0.211	0.98	
	17	−11.4	1.9	0.9	−3167.79	−6.939	0.211	0.98	
	18	32.4	1.84	0.985	−2930.39	−6.072	0.211	0.98	
	No.	t (°C)	p (bar)	Vapor fraction	h (kJ/kg)	s (kJ/kg·K)	m (kg/s)	Mole composition	
								N_2	O_2
Heat source fluid	19	465	1.043	1	459.725	1.081	7.58	0.79	0.21
	20	216	1.033	1	195.058	0.648	7.58	0.79	0.21
	21	145.9	1.023	1	122.915	0.491	7.58	0.79	0.21
	22	89.4	1.013	1	65.186	0.346	7.58	0.79	0.21

cess 1-2-3, the weak concentration solution in the power cycle 6-7-8-9-10-11, and the high concentration solution in the cooling cycle 14-15-16-17-18. The combined cycle also has four pressure levels: the high-pressure level (7-8) and low pressure level (9-10) in the power cycle, and the two intermediate pressure levels in the rectification process (2-3-4/12-⋯-6/14-15) and the refrigeration (16-17-18) and absorption processes (18/11-1).

The ammonia/water outflow from the absorber (point 1 in Fig. 1) is pumped to the rectification pressure (2). Before being fed to the rectifier, it is preheated by the external heat source to its saturation temperature (3). In the rectifier, this basic concentration solution is separated into a high concentration vapor (12) (almost pure ammonia) and low concentration solution (4), the first stream is sent to the condenser CON_2 and the second to the reboiler *REB*.

The weak solution from the reboiler (6) is brought into the power cycle by being pumped to the system high pressure level (7) and then evaporated and superheated by the heat source gas to the highest power cycle temperature (8). It then expands in the turbine to generate power (9). The condensed solution (10) from CON_1 is pumped to the absorption pressure and sent back to the absorber (11).

Table 3 The cogeneration system performance summary

Turbine (*T*) work (kW)		733.4
Pump work (KW)	(P_1)	2.2
	(P_2)	6.2
	(P_3)	0.2
Refrigeration output Q_{EVA} (kW)		241.9
Condenser (CON_1) load (kW)		1799.2
Rectifier condenser (CON_2) load (kW)		349.9
Cooler (*C*) load (kW)		50.1
Absorber (*ABS*) heat load (kW)		359.2
Boiler (*B*) heat input (kW)		2006.6
Reboiler (*REB*) heat input (kW)		547.0
Heat exchanger (*HEX*) heat input (kW)		437.7
Net power output *W* (kW)		724.9
Cooling/power ratio *R*		0.334
Heat input Q_{in} (kW)		3487.2
Exergy input E_{in} (kW)		1376.1
Energy efficiency η_I (%)		27.7
Exergy efficiency ε (%)		55.7

The high concentration saturated liquid (14) from CON_2 is subcooled in the heat exchanger *C* to (15). After being throttled in *V* to the refrigeration pressure (16), it provides refrigeration during its evaporation process in *EVA* (17), absorbs heat in the cooler *C* to (18), and finally it combines in the absorber (*ABS*) with stream (11) from the power cycle. The two streams mix there to form the basic concentration solution (1), which is cooled in *ABS* to its saturated state, and this completes the whole cycle.

The cycle can be heated by the flue gas of a gas turbine or any other industrial waste process heat with a suitable temperature, entering at 19. In this paper, the heat source fluid is chosen to be air (79% N_2 and 21% O_2). The hot air (19) flows through the hot sides of the boiler *B* (20), the reboiler *REB* (21), and the heat exchanger *HEX* (22) in turn, and is exhausted to the environment at the outlet of *HEX*.

In the two condensers CON_1 and CON_2, and the absorber *ABS*, the working fluid is cooled by 30°C water. This relatively high cooling water temperature was chosen to produce reasonably conservative performance results.

3 The Base-Case Cycle Performance

The system has two useful outputs: power and refrigeration. Since the heating fluid is finally exhausted to the environment, the calculation of the efficiencies is based on the initial state of the heating fluid. The energy efficiency is the ratio between the total energy outputs to the heat input from the heating fluid:

$$\eta_I = (W + Q_{EVA})/Q_{in} \tag{1}$$

where

$$Q_{in} = m_{hs}(h_{19} - h_a) \tag{2}$$

and where *W* is the power output from the turbine, reduced by the power input to the pumps (P_1, P_2 and P_3).

Since the energy efficiency weighs the power and refrigeration outputs as well as the heat input equally, even though the quality of these energies is rather different, exergy efficiency is a more proper evaluation criterion in this case, and in the evaluation of cogeneration systems with more than one kind of energy output or input in general.

The exergy efficiency is defined as the exergy output divided by the exergy input to the cycle:

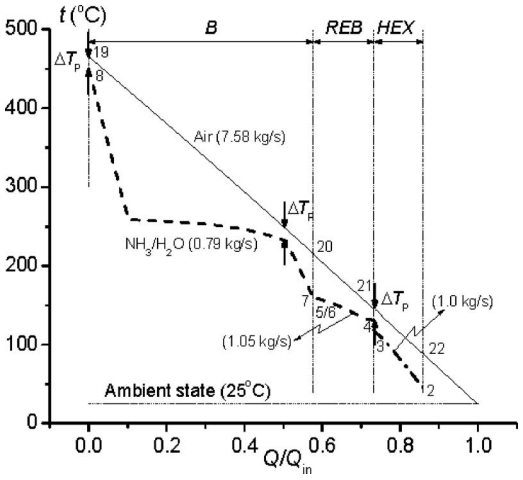

Fig. 2 The heat exchange *t-Q* diagram in the cogeneration cycle

$$\varepsilon = (W + E_{EVA})/E_{in} \tag{3}$$

where the exergy of the heating fluid, E_{in}, is given as:

$$E_{in} = m_{hs}[(h_{19} - h_a) - T_a(s_{19} - s_a)] \tag{4}$$

h_a and s_a are the enthalpy and entropy of the heat source fluid at ambient temperature and pressure. The exergy of refrigeration, E_{EVA}, is calculated as the exergy difference across the evaporator *EVA*

$$E_{EVA} = m_{16}[(h_{16} - h_{17}) - T_a(s_{16} - s_{17})] \tag{5}$$

It is assumed that the system operates at steady state. The simulations were carried out using the commercial Aspen Plus [19] code, in which the component models are based on the energy balance and mass balance, with the default relative convergence error tolerance of 0.01%; the thermal properties were calculated with the thermal property method of the Electrolyte NRTL model or the SR-Polar model for high temperature (>246°C) and pressure (>100 bar) application. To validate the property calculations, the property results from Aspen Plus and the data published by the International Institute of Refrigeration [20] were compared, and the results show good agreement between them.

The main assumptions for the calculations of the base case cycle are summarized in Table 1.

The proposed cogeneration system could be used as a bottom cycle in a combined cycle system, with a gas turbine as the topping cycle. Since the flue gas temperature of a common gas turbine of small size or middle size is about 500°C, the binary turbine inlet temperature is chosen to be 450°C in the base-case study, and it is varied in the study to investigate its effects on the system performance. Ammonia starts dissociating at higher temperatures to nitrogen and hydrogen, although some past studies (cf. [3]) have assumed its use in power cycles up to 532°C.

The calculations are based on unit mass flow rate (1.0 kg/s) of the basic working fluid fed to the rectifier. Table 2 summarizes the parameters, including temperature t, pressure p, vapor fraction, mass flow rate m, and ammonia mass fraction X, of some main streams of the cycle flow sheet.

The computed performance of the cycle is reported in Table 3. The exergy efficiency is much higher than the energy efficiency because the external heat source fluid is at a relatively low temperature and its exergy content is hence much lower than its energy content.

Figure 2 is the *t-Q* diagram of the cycle heat addition process. The heat duty Q is normalized by the cycle energy input Q_{in} (Eq. (2)), to show more clearly the fraction of heating fluid energy utilized in the system. To get a better temperature match with the heat source fluid, the positions of the boiler *B*, the reboiler *REB*, and the heat exchanger *HEX* are arranged according to their temperature levels. As shown in the figure, the minimal heat transfer temperature difference (15°C) appears at the hot end and the middle of the boiler, and at the cold end of the reboiler.

Table 4 The cycle exergy inputs, outputs, and losses decomposition (for m_1=1 kg/s)

		Amount (kW)	Percentage (%)
Exergy input	**Heat source**	**1376.13**	**100**
Exergy output	Power	724.88	52.68
	Refrigeration	41.78	3.04
	Sum	**766.66**	**55.72**
Exergy loss	CON_1	166.70	12.11
	B	149.44	10.86
	T	97.76	7.10
	ABS	40.95	2.98
	REB	40.63	2.95
	REC	20.77	1.51
	CON_2	17.51	1.27
	HEX	18.21	1.32
	C	4.93	0.36
	V	2.35	0.17
	P_2	1.93	0.14
	P_1	1.05	0.076
	P_3	0.084	0.006
	EVA	0	0
	Flue	46.95	3.41
	Sum	609.27	44.27

An exergy analysis was performed to evaluate the exergy losses in the system as shown in Table 4 and Fig. 3 and provide guidance for system improvement. The contribution of the cooling water exergy is not taken into account, because its exergy gain is lost to the environment anyway. Figure 3 demonstrates well how the exergy is used, lost, and reused in all of the system components. It was found that 44.3% of the total input exergy is lost: 3.4% to the environment in the flue, and 40.9% due to the irreversibilities in the components. The biggest exergy losses occur in the condensation process in CON_1 and the heat addition process in *B*; the exergy losses in these two components are nearly 23% of the total exergy input.

The exergy analysis results can now be used to guide system improvements. That condensation exergy loss (in CON_1) could be reduced if the heat transfer driving temperature difference could be reduced further; 1.7 percentage points of exergy efficiency increase can be expected for 5°C drop of the condensation temperature, but that would be at the expense of more costly heat exchangers. To reduce the exergy loss in the boiler *B*, a higher ammonia concentration in the working fluid is preferred to produce the desired temperature glide. However, it is hard to lower the turbine back pressure, because the higher concentration fluid requires a higher condensation pressure at the given temperature. There are ammonia concentrations that maximize the efficiencies, as discussed below.

The turbine expansion process causes the next largest exergy loss, which can be reduced by using a more efficient turbine. For example, the turbine can produce 5.8% more power if its isentropic efficiency increase to 92%, and the energy efficiency and exergy efficiency will increase to 28.9% and 58.8%, respectively, which means that a 3.1% reduction of overall exergy losses can be obtained by 5 percentage points increase of turbine isentropic efficiency. The exergy loss in *EVA* is 0, because the exergy associated with the refrigeration output is calculated as the working fluid exergy difference across the evaporator *EVA*.

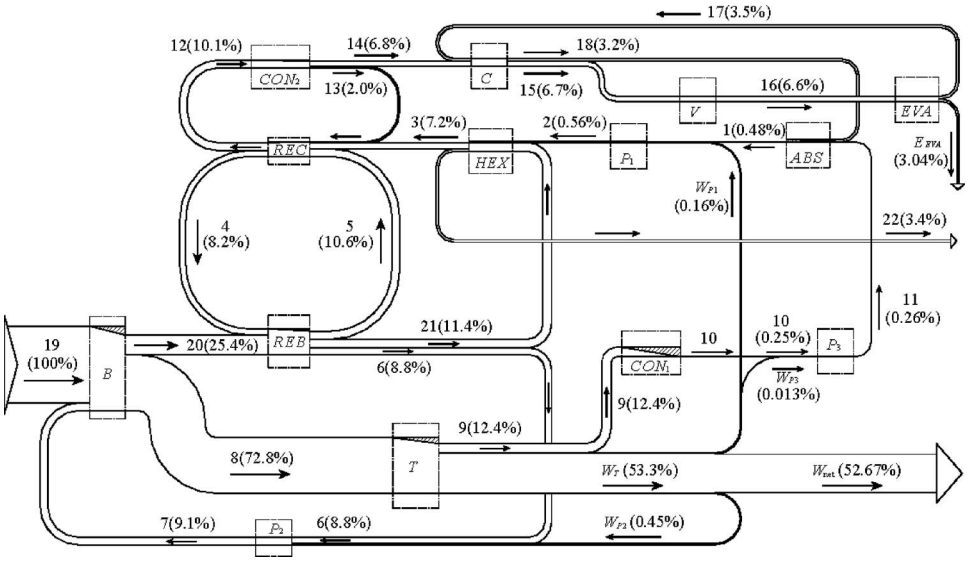

Fig. 3 The exergy flow diagram for the combined power/refrigeration cycle (the numbers are the fluid states, Fig. 1)

It is noteworthy that while the refrigeration *energy* output is about one third of the power output, its *exergy* value is only 5.8% of the power output, which indicates that the exergy efficiency values the cooling output only as a small contribution. This is partially because the refrigeration exergy is defined (Eq. (5)) as the minimal power needed to produce the refrigeration output Q_{EVA} in a reversible refrigeration cycle. In a practical system, much more power is needed to produce the same amount of refrigeration, because of the process irreversibilities [14,21].

The work demand to produce that cooling capacity Q_{EVA} in a reversible Carnot refrigeration cycle is:

$$W_{rev} = Q_{EVA}/COP_{rev} \tag{6}$$

and W_{rev} is equal to E_{EVA} defined in Eq. (5). The ratio $W_{rev}/Q_{EVA}=1/COP_{rev}$ is <0.2 for refrigeration produced above $-25\,^{\circ}\mathrm{C}$ and is only 0.17 for the base case cycle in this paper (with $T_a=(25+298.15)$ K).

Feeling that it under-represents the exergy of cooling, Vijayaraghavan and Goswami [14] proposed the use of $W=Q_{EVA}/COP_{practical}$ (instead of W_{rev} or E_{EVA}) as the refrigeration contribution in the exergy efficiency calculation. This would obviously result in a relatively larger exergy contribution of the produced refrigeration in this cogeneration system, and in a higher exergy efficiency than that calculated from Eq. (3), but presents a thermodynamic definition inconsistency. We therefore proceed with the definitions of Eqs. (3)–(5), keeping in mind that while the exergy input E_{in} in Eqs. (3) and (4) represents the *maximal* work that the heat input Q_{in} can produce, the refrigeration exergy output E_{EVA} represents the *minimal* work needed to produce the cooling energy Q_{EVA}.

4 Parametric Analysis and Discussion

In the power cycle, the turbine inlet temperature and pressure p_8 are independent variables. In all the calculations, the working fluid in the turbine is set to expand to the lowest possible pressure. When the pinch point temperature difference in the condenser is given, the turbine backpressure is determined just by the cooling water temperature and the working fluid concentration. In other words, the turbine backpressure p_b is not an independent variable, and the condenser outflow is the saturated liquid at the temperature that is the sum of the cooling water temperature and temperature difference needed for the heat transfer. Assumption of the rectifier feed (3) and the absorber outflow (1) being at saturation helps to reduce the number of independent variables.

In the rectifier there are several operation variables (such as the operation pressure, the reboiler outlet temperature, and the reflux ratio). Other cycle independent variables include the basic working fluid ammonia mass fraction, and the cooling water temperature.

Figure 4 shows the effect of the turbine inlet temperature t_8 (or the heating fluid inlet temperature t_{19}) on the cycle performance. These two temperatures are changed simultaneously to maintain the $15\,^{\circ}\mathrm{C}$ temperature difference at the boiler inlet.

It is clear from Fig. 4 that the increase of t_8 leads to the increase of the power output but has no impact on the refrigeration capacity. Therefore the refrigeration/power ratio decreases, and both energy and exergy efficiencies increase as well.

Since the bubble point temperature of the power cycle working fluid in the boiler *B* remains unchanged, when t_8 drops below about $450\,^{\circ}\mathrm{C}$, the heat transfer temperature differences in *REB* and *HEX* increase as a result, leading to the rapid increase of the heating fluid exhaust temperature and to the faster decrease of the efficiencies.

Figure 5 shows the effect of the turbine inlet pressure p_8. It has similar influence on the power and refrigeration outputs as that of the turbine inlet temperature, but milder. When p_8 is increased from 40 to 60 bar, the cooling capacity remains the same, the power output increases by 4.2%, and there is a pressure (about 52.4 bar in Fig. 5(*b*)), which maximizes the efficiencies.

Increasing the reboiler outlet temperature t_{REB} requires more heat input to the reboiler, which would increase the distillate rate and the refrigeration capacity. The reboiler temperature should not be lower than the bubble point temperature of the mixture; otherwise no distillate will be obtained at the top of the rectifier. Its upper limit is the temperature at which all the ammonia in the rectifier feed is distilled out. There are reboiler temperatures that maximize the energy and exergy efficiencies, since increasing t_{REB} beyond these values raises the reboiler heat input more than the consequent rise of the refrigeration capacity.

When the rectifier operation pressure p_{REC} increases, the distillate rate drops slightly. The refrigeration capacity decreases as a result; the power output remains almost unchanged. Both the energy and exergy efficiencies decrease. When p_{REC} drops below a

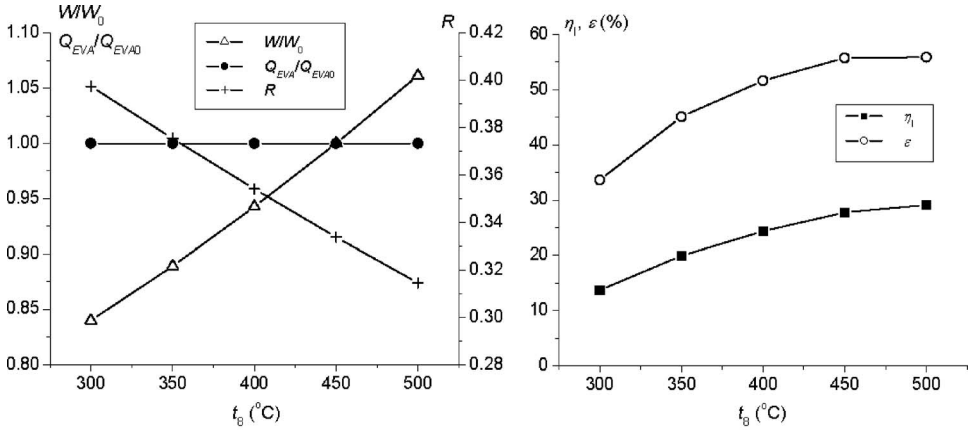

a. Normalized power output and refrigeration capacity

b. Thermal efficiency, exergy efficiency

Fig. 4 The effect of turbine inlet temperature, t_8

certain value, the distillate cannot be condensed for the given cooling water temperature, and hence no refrigeration will be produced.

As the rectifier molar reflux ratio *RR* increases, the distillate rate drops a little, but its ammonia concentration increases. The power output increases slightly. There are values of *RR* that maximize the efficiencies, which is about 0.3 for the exergy efficiency ε, and 0.2 for the energy efficiency η_I.

The effect of the basic ammonia mass fraction *X* in the working fluid (states 1-2-3) is shown in Fig. 6. When *X* increases, the mass flow rate of stream 14 increase too, leading to an increase of the refrigeration capacity and the decrease of the power output. The total output and the energy efficiency increase, since the refrigeration capacity increases faster. However, the rectifier feed temperature is lower for a higher ammonia concentration, thus more heat input is needed to drive the reboiler. It is found that there is an ammonia mass fraction that maximizes the exegy efficiencies ε, which are about 30% (Fig. 6(*b*)). The exergy efficiency drops afterwards because the drop of the power output dominates then.

There is an upper limit to *X*: if the concentration is too high, the working fluid cannot be condensed under the given pressure and cooling water temperature in the absorber.

The effect of the cooling water temperature is shown in Fig. 7. For a lower cooling water temperature, the working fluid in the turbine may expand to a lower pressure, therefore power output will increase, and so will the energy and exergy efficiencies. The refrigeration capacity remains unchanged because the ammonia is subcooled by the *EVA* outflow, instead of by cooling water in the heat exchanger *C*. From Fig. 7(*a*) we can conclude that when t_w is higher than 30°C, the rectifier operation pressure has to be increased so that the strong solution can be condensed in CON_2, and this leads to a dramatic decrease of the refrigeration capacity as t_w is raised. As seen from Fig. 7, when t_w drops from 40°C to 20°C, the power output increases by nearly 15%, the refrigeration capacity increases by 22%, the energy efficiency increases by 4.4 percentage points, and the exergy efficiency ε increases by 8.5 percentage points.

5 Comparison with Systems that Generate Power and Refrigeration Separately

In this section, the cogeneration system is compared with two other systems to meet the same power and refrigeration load. The first system is composed of a Kalina power cycle and a separate ammonia/water absorption refrigeration cycle. The second one is composed of a conventional steam Rankine cycle and a separate ammonia/water refrigeration cycle. In the two above options, the power cycle exhaust provides the heat to drive the refrigeration cycle. The comparison is made based on the same outputs as obtained for the above-analyzed power/refrigeration cogeneration cycle. The main parameters and performances of the three systems are summarized in the Table 5. The energy and exergy efficiencies

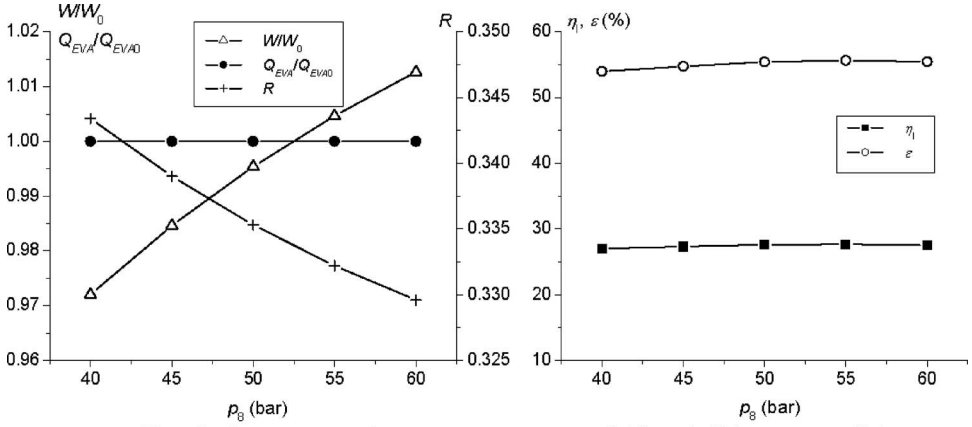

a. Normalized power output and refrigeration capacity

b. Thermal efficiency, exergy efficiency

Fig. 5 The effect of turbine inlet pressure, p_8

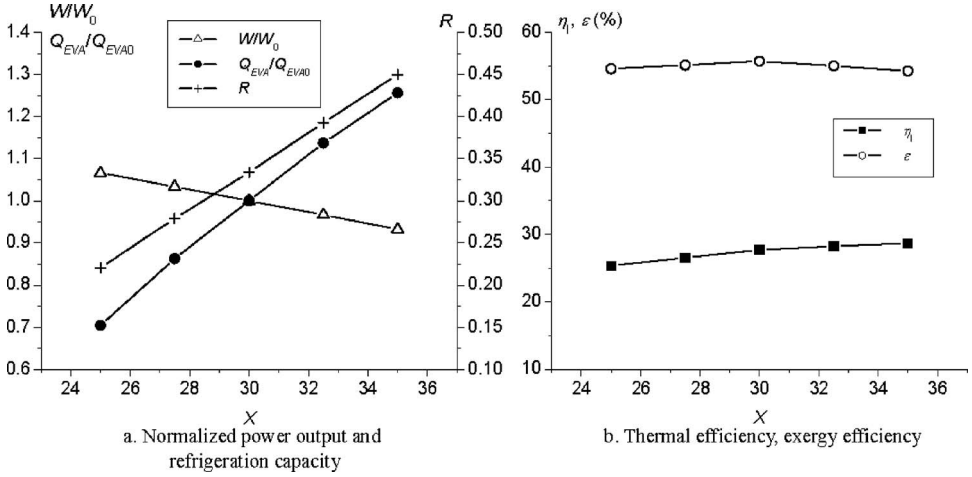

a. Normalized power output and refrigeration capacity

b. Thermal efficiency, exergy efficiency

Fig. 6 The effect of basic solution ammonia mass fraction, *X*

are used to evaluate the systems, instead of the *COP* (coefficient of performance) for the conventional analysis of a refrigeration system.

Figures 8 and 9 are the *t-Q* diagrams of the heat addition process when the power and refrigeration are generated by the above two cascade systems. The heat source fluid flows through the power and refrigeration cycles in a cascade, i.e., the same heating air releases heat first in the power cycle boiler and then in the refrigeration cycle reboiler.

As shown in Fig. 8 ("option 1"), a Kalina and absorption refrigeration cycle, the irreversibility in the heat transfer process is very large. The Kalina cycle heat addition process has a much higher NH_3 concentration ($X \approx 50\%$), and therefore has a steeper slope in the evaporation process, and could have thus perhaps by itself matched well with the heating fluid exothermic process. Since this process exists, however, together with the heat addition process in the refrigeration cycle reboiler, it does not have a good temperature match with the heating fluid. In other word, the advantage of a Kalina cycle cannot be realized in this cascade process.

In the Rankine cycle, the steam turbine has a much lower backpressure than the turbine with the binary working fluid, and thus its condensation process exergy loss is lower than that in the cogeneration system. However, the steam Rankine cycle evaporation process is isothermal, while the sensible heat source that provides the evaporation latent heat does it at a varying temperature, thus leading to large heat transfer related exergy destruction. Furthermore, the heat source fluid leaves the reboiler at a relatively higher temperature (146°C), resulting in a larger flue gas exergy loss to the environment. In the cogeneration system, the components are configured in a heat source to sink, temperature cascade. Specifically, to match with the heating fluid, the boiler was placed at the highest temperature region, followed by the reboiler. Lower in the cascade, the heating fluid at the outlet of the reboiler was used to preheat the working fluid feed to the rectifier, helping to reduce the reboiler load. The heat source fluid energy can thus be recovered more thoroughly, and its exhaust temperature is much lower (~90°C), leading to a markedly lower flue gas exergy loss than that in the two separate power and refrigeration generation systems proposed in this section for comparison. Since the component performances are all the same for the separate or cogeneration systems, the performance gain of the cogeneration system is mainly attributed to the system integration and better arrangement of internal mass and energy flows.

The cogeneration cycle is thus shown to have a much better performance in terms of both energy and exergy efficiencies. Compared to the two cascade generation systems, it requires a smaller heat source fluid mass flow rate. If the heat source is fuel, then the fuel consumption can be reduced significantly. Since the systems have the same power and refrigeration outputs, the energy consumption saving ratio is defined here as

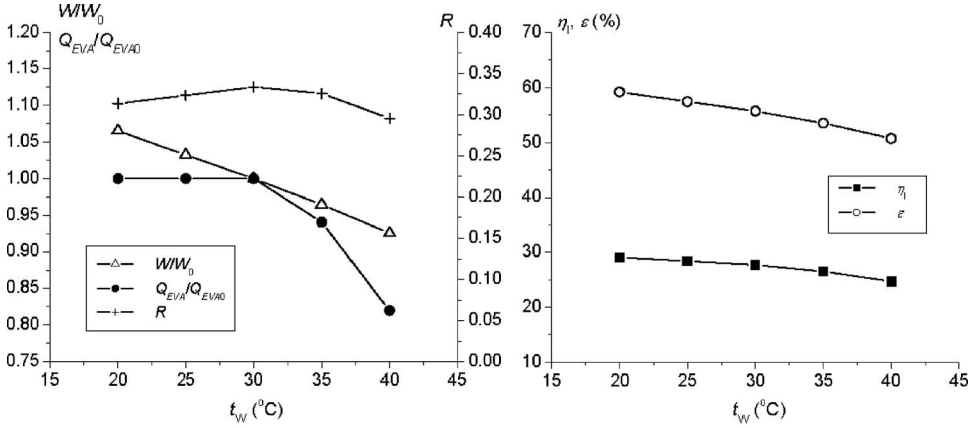

a. Normalized power output and refrigeration capacity

b. Thermal efficiency, exergy efficiency

Fig. 7 The effect of coolant cooling water temperature, t_w

Table 5 Comparison between the cogeneration and the separate power and refrigeration generation systems

			Option 1		Option 2	
		Cogeneration system	Kalina cycle	Refrigeration cycle	Steam Rankine cycle	Refrigeration cycle
Working fluid		Ammonia/water	Ammonia/water	Ammonia/water	Water	Ammonia/water
Working fluid mass flow rate (kg/s)		1.0	3.27	1.0	0.71	1.0
Turbine inlet temperature t_8 (°C)		450	450		450	
Turbine outlet back pressure p_b (bar)		0.242	1.26		0.09	
Turbine power output (kW)		733.44	737.37		732.21	
Cycle input (kW)	Reboiler (*REB*)	546.96		546.96		546.96
	Boiler (*B*)	2006.59	2923.77		2241.59	
	Heat exchanger (*HEX*)	437.67				
Cycle output (kW)	Cooling capacity Q_{EVA}	241.93	241.93		241.93	
	Net power output *W*	724.88				
		724.88				
		724.88				
Refrigeration/power ratio *R*		0.334	0.334		0.334	
Heat source fluid						
	Mass flow rate m_{hs} (kg/s)	7.58	10.30		8.28	
	Inlet temperature t_{19} (°C)	465	465		465	
	Exhaust temperature t_{22} (°C)	89.4	145.9		145.9	
Energy efficiency η_I (%)		27.72	20.4		25.38	
Exergy efficiency ε (%)		55.71	40.99		51.01	

$$ESR = (m_{hs,SP} - m_{hs,COG})/m_{hs,COG} \quad (7)$$

where $m_{hs,SP}$ and $m_{hs,COG}$ are the heating fluid mass flow rates of the cascade generation systems and of the cogeneration cycle, respectively. It is found that, compared with the system options 1 and 2, the *ESR*s of the cogeneration system are 35.9% and 9.2%, respectively.

Applying different flows to different section of the heat-absorbing components of the system allows adjustment of the driving temperature differences, and thus the exergy loss, through the system. Comparison with a separate steam Rankine cycle and a refrigeration cycle using different heating fluids in the power cycle and cooling cycle shows that the *ESR* of the cogeneration system is about 22% [22].

In the cogeneration system, the hardware used is conventional and commercially available. In addition, the power cycle and refrigeration cycle share some components, therefore some components necessary in the systems which generate power and refrigeration separately can be eliminated, making the cogeneration system more compact. For example, the flash tank, two absorbers, and the splitter in the Kalina cycle are not necessary in the cogeneration system; only the boiler, the turbine, and one condenser are added to the conventional absorption cycle.

6 An Alternative Configuration to Increase the Power Output

Higher turbine backpressures are desirable for reducing or preventing the potential for air leakage into the system, which would create problems in the operation or design of ammonia systems; a vacuum pump would be needed to extract the air and other noncondensable gases. At the same time, higher turbine pressure ratios raise the system power output and cycle efficiency. To seek the potential for thermal performance improvement, an alternative cycle configuration is investigated in this section, in which part of

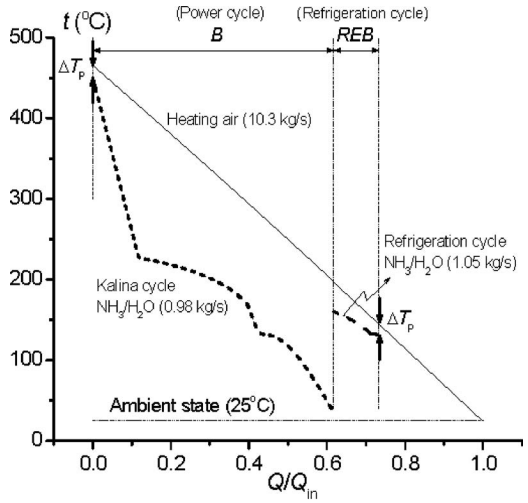

Fig. 8 The heat exchange *t-Q* diagram in the Kalina/refrigeration separate system (option 1)

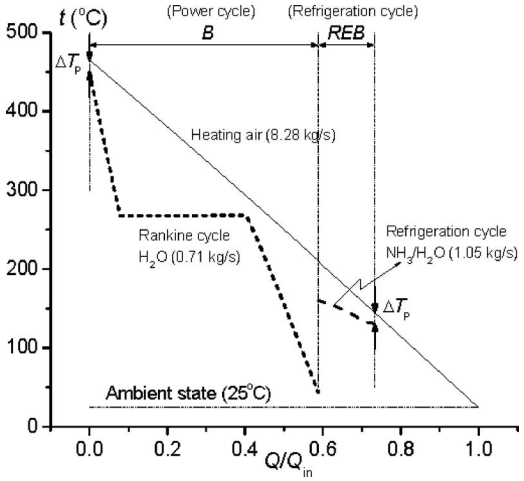

Fig. 9 The heat exchange *t-Q* diagram in the Rankine/refrigeration separate system (option 2)

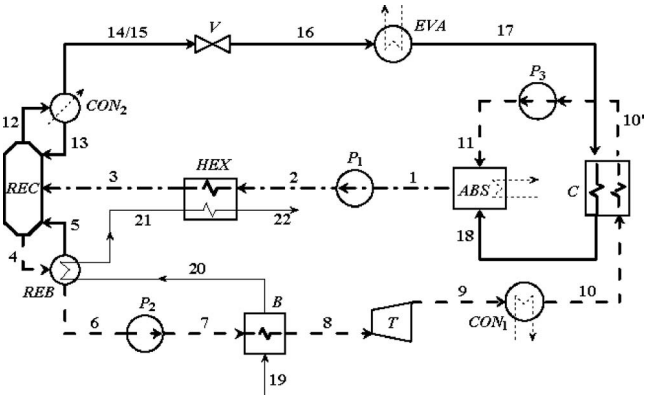

Fig. 10 The flow sheet of the alternative combined power/refrigeration cycle

the cooling from the refrigeration side is shifted to the power system side to reduce the turbine exhaust condensation temperature and thus the backpressure, too.

The cycle flow sheet is shown in Fig. 10. A heat exchanger (*C* in Fig. 10) is added before the absorber, in which the turbine exhaust is condensed to a lower temperature than that permitted by the cooling water. The strong ammonia solution outflow from the *EVA* provides the needed coldness to the condensation process. In this way, part of the refrigeration is transferred to the power output, and the turbine backpressure can be reduced to near the level of that in the conventional steam Rankine cycle. The minimum heat transfer temperature difference is set to be 5°C in this heat exchanger (*C*).

Figure 11 shows that as more coldness is moved to the power cycle (moving in the direction of lower turbine outlet back pressure p_b or the refrigeration/power ratio R), the cooling capacity drops and the power output increase (as expected), but their variations are not equal. When all of the refrigeration output is used to increase power output, the system will turn into a power cycle. From Fig. 11 it can be seen that decreasing the cooling capacity from 100% to 0% increases the power output by only 7.8%. It decreases the turbine exhaust back pressure from 0.242 bar in the base case to 0.128 bar, leading overall to a decrease of the thermal energy efficiency from 27.7% to 22.4%. R decrease from 0.334 to 0, and the exergy efficiency increases by nearly 1.1 percentage points. Work on further increase of power output and efficiencies requires cycle parameter optimization.

7 Some Considerations for Working Fluid Selection

The working fluid used in this type of cogeneration system is a binary mixture that must be suitable for use in absorption refrigeration cycles as well as in the power generation system. Much work has been done on identifying desirable properties of absorption cycle fluid pairs, and selecting or formulating various mixtures (cf. [23–26]).

In the absorption refrigeration cycle, the working fluid consists of two substances with different bubble point temperatures. They should not react chemically and have good solubility at the operation conditions. Besides the coefficient of performance of the refrigeration cycle, there are some other factors that need to be considered when choosing the refrigerant and absorbent (in part from [23–25]):

For the refrigerant:

(1) Proper operation pressures in both the evaporation and condensation processes: It is better that the evaporation pressure be higher than the ambient pressure, to avoid air inleakage. It also implies that the refrigerant should have a low boiling temperature at the ambient pressure. Also, the condensation pressure at ambient temperature should not be too high to reduce enclosure cost and out-leakage.
(2) High critical temperature and low freezing point temperature.
(3) High heat transfer coefficients.
(4) High specific refrigeration produced by unit refrigerant volume flow rate to reduce the plant size; low ratio of the solution (absorption reaction) heat to refrigerant latent heat, n_h

$$n_h = \frac{h_d}{r_o} \tag{8}$$

(lower solution heat requires more cooling of the absorber).
(5) Low heat exchange ratio n_L,

$$n_L \equiv fc(T_{GEN} - T_{ABS})/r_o \tag{9}$$

which is the ratio of the heat that has to be provided to the strong solution at generator inlet to bring it to equilibrium at the pressure and concentration, to the latent heat of evaporation. It determines the size of the heat exchanger between the weak and strong solution, and the possible efficiency loss due to the heat required in the generator to bring the strong solution to the equilibrium condition before desorption can start.
(6) Low viscosity to reduce the flow resistance, or a low pumping work ratio n_p

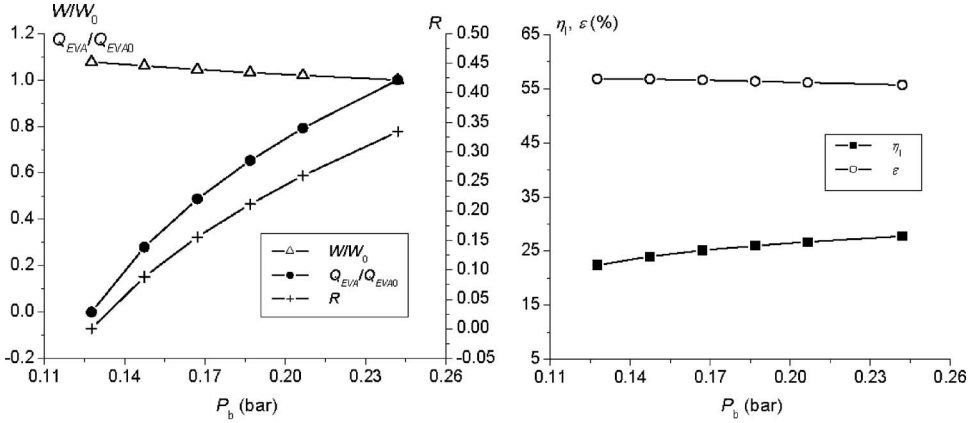

Fig. 11 Performance of the alternative cycle described in Fig. 10

$$n_p \equiv \frac{\text{pumping work}}{\text{latent heat of vaporization}} = \frac{f\Delta p}{\rho_L r_o} \tag{10}$$

where

$$f \equiv \frac{\text{rich solution mass flow rate}}{\text{pure refrigerant mass flow rate}} = \frac{1 - X_w}{X_r - X_w} \tag{11}$$

where X_r and X_w are the rich and weak solution concentrations, respectively, and Δp is the flow pressure difference.

Requirements (4)–(6) indicate the desirability of a solution with high r_o, ρ_L, X_r, and $(X_r - X_w)$, and low h_d, Δp, and c, recognizing, though, that some of these requirements are in conflict with each other.

For the absorbent:

(1) high absorbency with the refrigerant;
(2) much higher boiling temperature than that of the refrigerant at the same pressure; and both of them should also have
(3) no risk of crystallization,
(4) low corrosiveness and high stability (chemically and thermally) in the operation region,
(5) low toxicity and flammability,
(6) low price and good availability.

In cogeneration systems, the absorbent (with lower concentration of refrigerant) should be also suitable for use in the power cycle (specifically Rankine cycle in this case), and thus must have some other properties:

(1) to be condensed by ambient cooling water or air, its critical temperature must be higher than the ambient temperature;
(2) high specific power production per unit working fluid mass flow rate;
(3) high stability in the high temperature range at which it is heated (400–500 °C here), noting that the power cycle typically operates at a higher top temperature than the refrigeration cycle;
(4) high density at the final expansion stage (to reduce the size of turbine blades in the last stages);
(5) low back-work ratio;
(6) properties that promote high heat transfer coefficients in the power cycle heat exchangers such as boiler, condenser, regenerators, etc.

The ammonia water mixture was chosen as the working fluid in this study because (1) it is one of the most commonly used working media in absorption refrigeration systems and can produce refrigeration in the wide temperature range of −50–10 °C, (2) the boiling temperature profile makes it possible to get a good thermal match with sensible heat sources, and (3) the system can use low/medium temperature heat sources, such as waste, solar, and geothermal. Except for its toxicity and flammability, ammonia has many merits: it is widely available, inexpensive, has high specific refrigeration production per unit mass flow rate, low viscosity, and good heat transfer performance. It has proper evaporation and condensation pressures; for example, the evaporation pressure is above ambient pressure with refrigeration produced at −33 °C, and the condensation pressure is usually 12–14 bar.

At the same time, water is the most common working fluid in power plants. It offers a very low back-work ratio, is safe and cheap. Rich experience has been accumulated in running steam Rankine power cycles.

Literally thousands of fluid pairs were considered or studied for absorption refrigerators and heat pumps to come up with better alternatives than the commonly used NH_3-H_2O and $H_2O-LiBr$, to overcome some of the shortcomings of these pairs and to introduce new applications where these fluids are inadequate (cf. [23–26]). These include both inorganic and organic fluids, and the studies focus on (1) additives to existing fluids, (2) modifications or substitutions of existing fluids, (3) screening of new fluids, and (4) synthesis of new fluids. Leading among the inorganic fluids considered are still ammonia refrigerant with absorbents such as water with various salts such as $H_2O-LiBr$, $CaCl_2$, LiSCN, and NaSCN; water as refrigerant with LiBr, LiBr-ethylene glycol, zeolites, H_2SO_3, and others; H_2O-CH_3OH refrigerant with LiBr; CO_2 refrigerant with aqueous amines, and others. Among the organic fluids are fluorinated refrigerants (now restricted to a small number because of the ozone problem) with various organic absorbents, methyl alcohol refrigerant with various inorganic salts as absorbents, and methalamine refrigerant with various salts, water, or organic absorbers. It is noteworthy that some of these fluids are also associated with power generation systems being developed for reducing CO_2 emissions, and useful synergies may be found. Detailed studies for finding new fluid pairs and the impact of their properties on cogeneration system performance are absent and much recommended.

8 Concluding Remarks

A new ammonia-water system is proposed for the cogeneration of refrigeration and power. The energy and exergy efficiencies were found to be 27.7% and 55.7%, respectively, in the base case with the maximum cycle temperature of 450 °C. The exergy analysis shows that conventional improvements in the condenser and other heat exchangers as well as in the turbine efficiency can raise the exergy efficiency to over 60%. The parametric study shows that increasing the turbine inlet temperature has positive effects, whereas increasing the rectifier operation pressure has a negative effect and that there exist turbine inlet pressures, reboiler temperatures, rectifier reflux ratios, and ammonia concentrations that maximize the energy and exergy efficiencies. Comparison with other optional systems for separate generation of power and refrigeration having the same power output and refrigeration capacity shows that the cogeneration system has higher energy and exergy efficiencies: its energy consumption is lower by more than 36% and 9% than the two separate power and cooling cascade systems analyzed for comparison.

One feature of the binary working fluid is that the cycle condensation takes place at a varying temperature too, resulting in a turbine backpressure that is usually higher than that in the steam Rankine cycle. Higher backpressure is good to prevent air leakage into the system, but unfavorable to the power output and efficiency. By coupling further with the refrigeration cycle, the power cycle condensation process can be achieved at a pressure and temperature much lower than those in the conventional binary cycle with the same working fluid. The cycle pressure ratio and thermal performance can thereby be increased accordingly; and the combined cycle refrigeration/power ratio can be varied too since part of the cooling duty is transferred to the power output. Here, dropping the turbine pressure from 0.242 bar in the base case to 0.128 bar, the power output increases by 8%, the exergy efficiency increases by nearly 1.1 percentage points, and the refrigeration/power ratio decreases from 0.334 to 0, thereby shifting all the refrigeration output to power.

A brief review of desirable properties of fluid pairs for such cogeneration cycles was made, and detailed studies for finding new fluid pairs and the impact of their properties on cogeneration system performance are absent and are very recommended.

Acknowledgment

The first author gratefully acknowledges the support of the Chinese Natural Science Foundation Project (No. 50576096).

Nomenclature

COP = coefficient of performance
c = specific heat (kJ/(kg·K))
E = exergy (kW)
ESR = energy saving ratio

f = specific solution circulation rate
h = specific enthalpy (kJ/kg)
h_d = heat of the absorption reaction (kJ/kg)
m = mass flow rate (kg/s)
n_h = reaction to latent heat ratio
n_L = heat exchange ratio
n_p = pumping work to vaporization latent heat ratio
p = pressure (bar)
p_b = turbine backpressure (bar)
Q = heat duty (kW)
r_o = latent heat of evaporation of the refrigerant (kJ/kg)
R = refrigeration/power ratio
RR = rectifier molar reflux ratio
s = specific entropy (kJ/kg·K)
T = temperature (K)
t = temperature (°C)
VF = vapor fraction
W = power output (kW)
X = ammonia mass fraction (kg ammonia/kg mixture)

Greek

Δp = pressure difference (bar)
ΔT_P = pinch point temperature difference (K)
η_I = energy (first law) efficiency
ε = exergy efficiency

Subscripts

a = ambient state
ABS = absorber
B = boiler
COG = cogeneration
EVA = evaporator
GEN = generator
HEX = heat exchanger
hs = heat source fluid
in = input
r = rich solution
rev = reversible
REB = reboiler
SP = separate generation
w = weak solution
0 = base case
1, 2,…,22 = states on the cycle flow sheet

References

[1] Horlock, J. H., 2003, *Advanced Gas Turbine Cycles*, Pergamon, Oxford.
[2] Maloney, J. D., and Robertson, R. C., 1953, "Thermodynamic Study of Ammonia-Water Heat Power Cycles," ORNL Report No. CF-53-8-43, Oak Ridge, TN.
[3] Kalina, A. I., 1984, "Combined-Cycle System with Novel Bottoming Cycle," ASME J. Eng. Gas Turbines Power, **106**, pp. 737–742.
[4] Ibrahim, O. M., and Klein, S. A., 1996, "Absorption Power Cycles," Energy, **21**(1), pp. 21–27.
[5] Gao, L., Wang, Y., Jin, H., Liu, Z., and Cai, R., 2002, "A Novel Binary Cycle With Integration of Low-Level Waste Heat Recovery and LNG Cold Energy Utilization," J. Eng. Thermophys., **23**, pp. 397–400 (in Chinese with English abstract).
[6] Wang, Y., Han, W., Jin, H., and Zheng, D., 2003, "A Novel Binary Cycle with Mid and Low Temperature Heat Recovery," Proc. Chin. Soc. Electr. Eng., **23**, pp. 200–204 (in Chinese with English abstract).
[7] Horlock, J. H., 1987, *Cogeneration-Combined Heat and Power (CHP)—Thermodynamics and Fluid Mechanics Series*, Pergamon, Oxford.
[8] Goswami, D. Y., 1998, "Solar Thermal Technology: Present Status and Ideas for the Future," Energy Sources, **20**, pp. 137–145.
[9] Goswami, D. Y., and Xu, F., 1999, "Analysis of a New Thermodynamic Cycle for Combined Power and Cooling Using Low and Mid Temperature Solar Collectors," ASME J. Sol. Energy Eng., **121**, pp. 91–97.
[10] Hasan, A. A., and Goswami, D. Y., 2003, "Exergy Analysis of a Combined Power and Refrigeration Thermodynamic Cycle Driven by a Solar Heat Source," ASME J. Sol. Energy Eng., **125**, pp. 55–60.
[11] Lu, S., and Goswami, D. Y., 2003, "Optimization of a Novel Combined Power/Refrigeration Thermodynamic Cycle," ASME J. Sol. Energy Eng., **125**, pp. 212–217.
[12] Tamm, G., Goswami, D. Y., Lu, S., and Hasan, A. A., 2003, "Novel Combined Power and Cooling Thermodynamic Cycle for Low Temperature Heat Sources, Part 1: Theoretical Investigation," ASME J. Sol. Energy Eng., **125**, pp. 218–222.
[13] Tamm, G., and Goswami, D. Y., 2003, "Novel Combined Power and Cooling Thermodynamic Cycle for Low Temperature Heat Sources, Part 2: Experimental Investigation," ASME J. Appl. Mech., **125**, pp. 223–229.
[14] Vijayaraghavan, S., and Goswami, D. Y., 2003, "On Evaluating Efficiency of a Combined Power and Cooling Cycle," ASME J. Energy Resour. Technol., **125**, pp. 221–227.
[15] Zheng, D., Chen, B., and Qi, Y., 2006, "Thermodynamic Analysis of A Novel Absorption Power/Cooling Combined Cycle," *Proceedings of ISHPC'02*, Applied Energy, Vol. 83, pp. 311–323.
[16] Erickson, D. C., 1989, "Absorption Heat Pumped Co-generation Engine—Includes Absorption and Desorption Heat Exchangers for Low Pressure Steam and Exhaust Gas," U.S. Patent 48,03,958-A; International Publication Number WO8902563-A.
[17] Erickson, D. C., 2004, "Integrated Steam-Ammonia Power Cycle for a Gas Turbine Combined Cycle Plant Comprises a Steam Condenser, an Ammonia Superheater, a Feed Water Preheater and an Ammonia Feed Preheater," U.S. Patent 2004139747-A1; International Publication Numbers WO2004067918-A2; US6895740-B2.
[18] Erickson, D. C., and Anand, G., 2001, "Absorption Power Cycle for Converting Thermal Energy to Mechanical Energy, has Separate Pumps for Pumping Weak Absorbent to Different Sections of High Pressure Generator," U.S. Patent US6269644-B1; International Publication Number WO200194757-A1.
[19] Aspen Plus®, Aspen Technology, Inc., version 11.1, http://www.aspentech.com/.
[20] International Institute of Refrigeration, 1994, "Thermodynamic and Physical Properties NH_3–H_2O."
[21] Lior, N., and Zhang, N., 2005, "Energy, Exergy, and Second Law Performance Criteria," *Proc. ECOS2005*, NTNU, Trondheim, Norway, p. 437–445, and revised version in 2007, Energy, 32, pp. 281–296.
[22] Zhang, N., Cai, R., and Lior, N., 2004, "A Novel Ammonia-Water Cycle for Power and Refrigeration Cogeneration," ASME Paper No. IMECE2004–60692.
[23] Hodgett, D. L., 1982, "Absorption Heat Pumps and Working Pair Developments in Europe since 1974, in New Working Pairs for Absorption Processes," Proc. Workshop, W. Raldow, Ed., Berlin, Germany, April 14–16, Swedish Council for Building Research, Stockholm, Sweden, pp. 57–70.
[24] Ryan, J. D., 1983, "Fluid Pairs for Advanced Absorption Cycles: Selection Methods and Data Requirements," 18th IECEC, Paper No. 839313, pp. 1915–1920.
[25] Raldow, W., ed., 1982, "New Working Pairs for Absorption Processes," Proc. Workshop, Berlin, Germany, April 14–16, Swedish Council for Building Research, Stockholm, Sweden.
[26] Macriss, R. A., and Zawacki, T. S., 1989, "Absorption Fluids Data Survey: 1989 Update," Report ORNL/Sub/-84-47989/4, Oak Ridge National Laboratory, Oak Ridge, TN.

Dr. Na Zhang *is a research professor at the Institute of Engineering Thermophysics. Chinese Academy of Sciences (CAS). She obtained her Ph.D. in Engineering from the same institute in 1999. She is an associate editor of Energy—The International Journal. Her major research works include gas turbine and combined cycle, cogeneration system, coal-fired power system,* CO_2 *capture from power plant, and power generation with LNG cold exergy. She has published approximately 80 scientific papers.*

Noam Lior *(Ph.D., University of California, Berkeley; Fellow ASME; Associate Fellow AIAA) is a Professor of Mechanical engineering and Applied Mechanics at the University of Pennsylvania with extensive experience in heat and mass transfer, thermodynamics, fluid mechanics, energy power, and water desalination education and consulting. He is Editor-in Chief of Energy, The International Journal, 1998–current; Regional Editor for North America and Europe, Energy Conversion and Management Journal; Board of Editors Member, Desalination; Technical Editor, ASME Journal of Solar Energy Engineering, 1983-1989; Editor, Thermal Science and Engineering journal (Japan), 1999; and Editor-in-Chief, Advances in Water Desalination book series, John Wiley, 2006–. He has more than 200 technical publications.*